Cite This: *Inorg. Chem. XXXX, XXX, XXX–XXX*

Copper²⁺ Binding to α-Synuclein. Histidine50 Can Form a Ternary Complex with Cu²⁺ at the N-Terminus but Not a Macrochelate

Yao Tian,[∥,†] Helen F. Stanyon,[∥,†] Joseph D Barritt,[∥,†,‡] Uroosa Mayet,[†] Pelak Patel,[†] Elena Karamani,[†] Giuliana Fusco,[§] and John H. Viles*,[†]

[†]School of Biological and Chemical Sciences, Queen Mary, University of London Mile End Road, London E1 4NS, United Kingdom
[‡]Department of Life Sciences, Imperial College London, London SW7 2AZ, United Kingdom
[§]Centre for Misfolding Diseases, Department of Chemistry, University of Cambridge, Cambridge CB1 1EW, United Kingdom

ⓈⓈ *Supporting Information*

ABSTRACT: α-Synuclein (αSyn) forms amyloid fibrils in the neurons of Parkinson's disease (PD) patients'. Despite a role for Cu²⁺ in accelerating αSyn fibril formation, coupled with reports of copper dis-homeostasis in PD, there remain controversies surrounding the coordination geometry of Cu²⁺ with αSyn. Here we compare visible circular dichroism (CD) spectra of Cu²⁺ loaded on to full-length αSyn together with four peptides that model aspects of Cu²⁺ binding to the N-terminus and histidine50 of αSyn. With glycine as a competitive ligand, the affinity of Cu²⁺ for full-length αSyn is determined to have a conditional dissociation constant, at pH 7.4, of 0.1 nM. A similar affinity of 0.3 nM is determined for the tripeptide Met-Asp-Val(MDV) that mimics the N-terminus of αSyn, while the incorporation of a putative histidine side chain in the N-terminal complex facilitates the formation of a macrochelate with the histidine, which results in an

increase in the affinity for Cu²⁺ to 0.03 nM at pH 7.4. Comparisons of the visible absorbance and CD spectra over a range of pH values also indicates that the MDV tripeptide closely models Cu²⁺ binding to full-length αSyn and rules out a role for His50 in the primary Cu²⁺ binding complex of monomeric αSyn. However, there are reports that suggest His50 does form a macrochelate with the N-terminal Cu²⁺ complex; we reconcile these conflicting observations by identifying a concentration dependence of the interaction. Only at the higher concentrations can the imidazole nitrogen bind to the N-terminal Cu²⁺ to form a ternary complex rather than via a macrochelate. This work shows even for this intrinsically disordered protein a large macrochelate with Cu²⁺ is not favored. Understanding Cu²⁺ coordination to αSyn gives a more complete picture of its place in amyloid assembly and cytotoxicity.
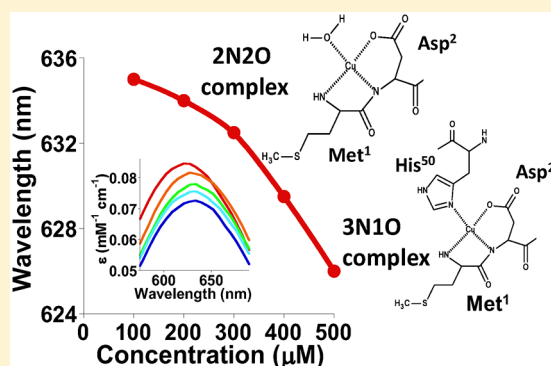
INTRODUCTION

Parkinson's disease (PD) is the second most prevalent neurodegenerative disorder after Alzheimer's disease. PD is marked by the loss of dopaminergic neurons in the brain's *substantia nigra*, along with the presence of subcellular protein accumulations, known as Lewy bodies. These Lewy bodies are comprised of amyloid fibrils of the protein α-synuclein (αSyn). Furthermore, some early-onset inherited forms of PD are associated with single-point mutations within αSyn, for example, A53T, A30P, E46K, and H50Q.[1] Metal ions, and, in particular, copper ions, have been linked with PD through the observation of increased Cu²⁺ concentrations in the cerebrospinal fluid of PD patients,[2] while those with chronic exposure to copper in industry have an increased risk of developing PD.[3]

αSyn is largely found intracellularly at presynaptic terminals in the reducing environment of the cytosol, where copper ions are predominantly Cu⁺. There have been a number of studies of Cu⁺ coordination to αSyn.[4a−c] In addition, Cu ions are

capable of redox cycling between Cu⁺ and Cu²⁺, which can lead to hydroxyl radical production and other reactive oxygen species, a hallmark of PD.[5] Indeed, hydroxyl radical production by copper redox cycling can cause dityrosine formation in αSyn, which can affect amyloid assembly.[6] A proportion of αSyn is secreted by neuronal cells extracellularly,[7] which highlights the importance of Cu²⁺ binding to αSyn.

The coordination of Cu²⁺ can affect the structure and self-assembly of αSyn. The change in charge may affect the self-association, while Cu²⁺ coordination can affect the amyloid assembly pathway[8] and structural morphologies (strain) of the amyloids fibrils.[9] Cu²⁺ has been proposed as a trigger for the misfolding and assembly of αSyn in PD, as Cu²⁺ can accelerate αSyn fibril formation in vitro.[8,9c,10] Cu²⁺ has also been shown to exacerbate toxicity of oligomeric αSyn in cell cultures.[9b,c] It is for these reasons much effort has been directed at

characterizing the coordination and affinity of Cu^{2+} binding to αSyn; for reviews, see refs 4b, c, and 11.

Visible circular dichroism (Vis-CD) is a powerful probe of coordination in metal ion–protein complexes. The coordination of Cu^{2+} via amide main-chain chelation generates CD signal in the d–d electronic absorption bands, known as the vicinal effect. The sign of the signal is very sensitive to the coordination geometry.[12] One advantage Vis-CD has over visible absorption spectra is that the nonprotein bound metal ion is typically CD silent. As a consequence, determination of the stoichiometry, coordination geometry, and pH dependence of metal ion binding is not complicated by signal from the free metal ion.[10a,13]

αSyn is 140 residues in length and is intrinsically disordered in an aqueous environment. Paramagnetic broadening by Cu^{2+} of ^{1}H–^{15}N HSQC NMR spectra of full-length αSyn identified three regions of the protein that interact with Cu^{2+} ions. These were centered at the N-terminus, His50 and Asp121,[10a,14] although paramagnetic broadening by Cu^{2+} can be caused by weak transient Cu^{2+} binding. Numerus studies have now shown the locus of the primary binding site for Cu^{2+} to be the N-terminal amino group.[4b] These include spectroscopic[15,16] and potentiometric studies[15b,16d] of peptide models and comparisons with full-length αSyn. It has been suggested that αSyn binds Cu^{2+} ions through two different modes, solely at the N-terminal residues Met-Asp-Val (MDV), see Figure 1a,[15] or alternatively, via the N-terminal residues together with

the imidazole of histidine at position 50 to form a macrochelate complex, Figure 1b,[16] while model peptides of the N-terminus (MDV), together with free imidazole, have been shown to form a ternary Cu^{2+} complex at high pH.[17] Post-translational modifications of αSyn where the N-terminus becomes acetylated have been reported.[18,19] Although quantitation is difficult, the acetylation of the N-terminus is believed to be quite widespread, but it is not thought to be universal. The primary binding site for Cu^{2+} for acetylated αSyn is centered at His50 not at the N-terminal residues.[20]

We aim to build on the large body of work surrounding the coordination of Cu^{2+} to αSyn and resolve some of the controversies surrounding the role of His50 in the primary N-terminal binding site. To investigate the influence of the side chains Asp2 and His50 on Cu^{2+} binding to the N-terminus of αSyn, four peptide models were generated: (i) αSyn(1–3) (MDV-am); (ii) αSyn(1–3D2A) (MAV-am); (iii) αSyn-(ac46–52) (ac-EGVVHGV-am); and (iv) αSyn(1–7,46–52) (MDVFMKGEGVVHGV-am). The affinities, visible-CD, absorption spectrum, and pH dependence of coordination are directly compared with Cu^{2+} binding to full-length αSyn. We show the affinity, pH dependence, absorbance, and visible-CD spectra for full-length, αSyn is most similar to that of the tripeptide MDV, and the histidine side chain at position 50 does not coordinate to the primary Cu^{2+} binding site in full-length αSyn by forming a macrochelate.

■ EXPERIMENTAL SECTION

Expression and Purification of αSyn. αSyn was expressed and purified as previously described.[21] Briefly the protein was expressed in *Escherichia coli* using plasmid pT7–7.[21] After it was transformed in BL21 (DE3)-gold cells (Agilent Technologies), αSyn was obtained by growing the bacteria in luria broth (LB) at 37 °C under constant shaking at 250 rpm and supplemented with 100 μg·ml^{-1} ampicillin to an OD of 0.6. The expression was induced with 1 mM isopropyl β-D-1-thiogalactopyranoside (IPTG) at 37 °C for 4 h, and the cells were harvested by centrifugation at 6200g (Beckman Coulter). The cell pellets were resuspended in lysis buffer (10 mM Tris-HCl pH 8, 1 mM ethylenediaminetetraacetic acid (EDTA) and EDTA-free complete protease inhibitor cocktail tablets obtained from Roche) and lysed by sonication. The cell lysate was centrifuged at 22 000g for 30 min to remove cell debris. To precipitate the heat-sensitive proteins, the supernatant was then heated for 20 min at 70 °C and centrifuged at 22 000g. Subsequently streptomycin sulfate was added to the supernatant to a final concentration of 10 mg·ml^{-1} to stimulate DNA precipitation. The mixture was stirred for 15 min at 4 °C followed by centrifugation at 22 000g. Then, ammonium sulfate was added to the supernatant to a concentration of 360 mg·ml^{-1} to precipitate the protein. The solution was stirred for 30 min at 4 °C and centrifuged again at 22 000g. The resulting pellet was resuspended in 25 mM Tris-HCl, pH 7.7, and dialyzed against the same buffer to remove salts. The dialyzed solutions were then loaded onto an anion exchange column (26/10 Q sepharose high performance, GE Healthcare) and eluted with a 0–1 M NaCl step gradient, and then further purified by loading onto a size exclusion column (Hiload 26/60 Superdex 75 preparation grade, GE Health-care). All the fractions containing the monomeric protein were pooled together and concentrated by using Vivaspin filter devices (Sartorius Stedim Biotech). The purity of the aliquots after each step was analyzed by sodium dodecyl sulfate–poly(acrylamide) gel electrophoresis (SDS-PAGE), and the protein concentration was determined from the absorbance at 275 nm using an extinction coefficient of 5600 M^{-1} cm^{-1}.

Peptides and Proteins. Peptides were purchased from Generon Ltd. F-moc chemistry was used to synthesize the various model peptides. All peptides were C-terminally amidated to mimic the continuation of the peptide sequence in the larger protein. The
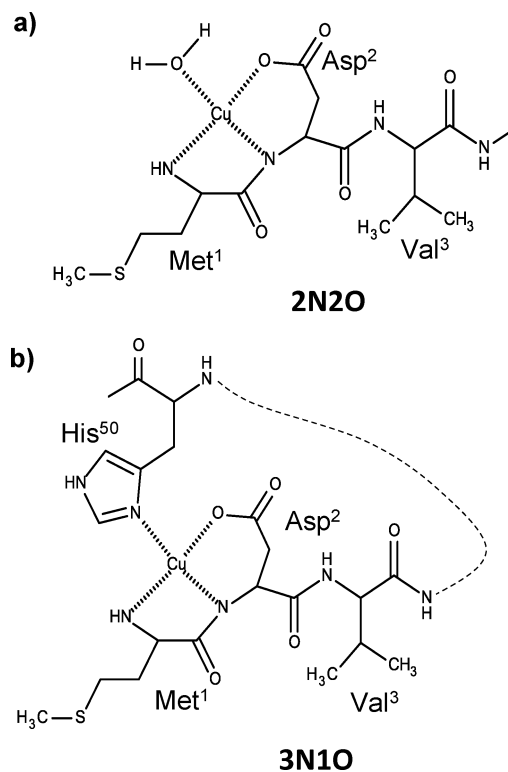

Figure 1. The proposed primary tetragonal Cu^{2+} coordination geometries of αSyn. The coordination geometries of Cu^{2+} binding to αSyn via (a) 2N2O-mode; the N-terminal amino nitrogen, the amide nitrogen of Asp2, the carboxylate oxygen of the Asp2 side-chain, and an oxygen from water {NH$_2$; N$^-$; β-COO$^-$; H$_2$O} and (b) 3N1O-mode, where the water oxygen is replaced by an imidazole nitrogen of His50 to form a macrochelate {NH$_2$; N$^-$; β-COO$^-$; N$_{Im}$}.
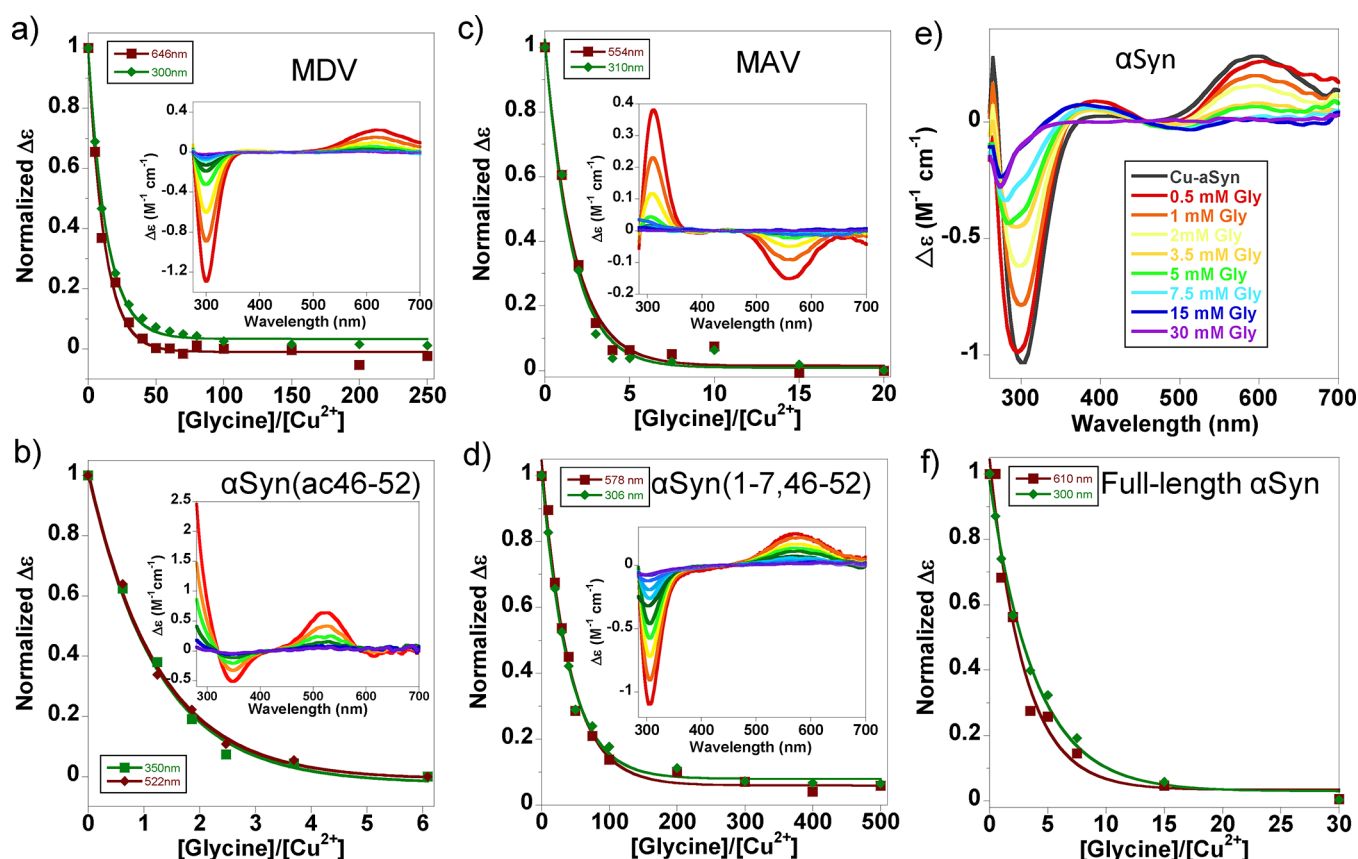
Figure 2. The affinity of Cu²⁺ binding to α-synuclein and peptide models. Vis-CD spectra of glycine competition in the presence of 1 mol equiv of Cu²⁺ ions at pH 7.4, together with glycine competition binding curves. (a) MDV at 500 μM; (b) αSyn(ac46−52) at 100 μM; (c) MAV at 500 μM; (d) αSyn(1−7,46−52) at 300 μM; (e, f) full-length αSyn at 100 μM with glycine competition binding curves.

peptides were removed from the resin and deprotected before purification to a single elution band by reverse-phase high-performance liquid chromatography (HPLC). The samples were characterized using mass spectrometry (MS).

Peptides with amidated C-termini (am) and free N-terminal amino groups studied included MDV, MAV, ac-EGVVHGV (with acetylated N-terminus; αSyn(ac46−52)), and MDVFMKGEGVVHGV; a designed sequence based on α-synuclein residues 1−7 and 46−52; αSyn(1−7,46−52).

UV−Visible Absorption Spectroscopy. UV−Visible electronic absorption spectra of the Cu²⁺ complexes were acquired using a Hitachi U-3010 spectrophotometer using a 1 cm path-length (l) quartz cuvette. Spectra were acquired between 200 and 800 nm with a wavelength scan speed of 60 nm mins⁻¹. Absorption spectra were smoothed using a 6 nm window and adjusted for concentration (c); ε = Abs/($c \times l$) (Abs = absorbance).

Circular Dichroism (CD). Typically, CD spectra were recorded at 25 °C on an Applied Photophysics Chirascan instrument between 260 and 800 nm, with sampling points every 2 nm, using a 1 cm path length cell. Typically, three scans were recorded and averaged, baseline spectra subtracted from each spectrum, followed by smoothing using a window of 6 nm. Data were processed using Applied Photophysics Chirascan Viewer, Microsoft Excel and the KaleidaGraph spreadsheet/graph package. The molar ellipticity Δε (M^{-1} cm^{-1}) spectra were obtained through conversion of the direct CD measurements (θ, in millidegrees), using the relationship $\Delta\varepsilon = \theta/(c \times l \times 33\,000)$, where c is the molar concentration, and l is the path-length.

Titrations. All chemicals were purchased from Sigma-Aldrich at the highest purity available, and double distilled water was used throughout (1×10^{-18} Ω^{-1} cm^{-1} resistivity). Small aliquots of fresh 20 mM aqueous solutions (Cu²⁺ as CuCl₂·2H₂O) and glycine were used for titrations. Typically ethylmorpholine buffer (20 mM) was

used in most measurements while pH dependence titration spectra were recorded in the absence of a buffer. The pH was adjusted with microliter additions of 0.05 mM NaOH or HCl. pH was maintained to within 0.05 of a pH unit. The pH was measured before and after acquisition of each spectrum. The lyophilized weight of each peptide was used to estimate the concentration, assuming 20% moisture content. However, it was the known concentration of metal ions at sub-stoichiometric levels to the peptide that was used for the conversion to molar ellipticity.

Affinity Measurements. Glycine, the competing Cu²⁺ chelator used in calculating the affinity of the Cu²⁺−peptide complexes, forms a Cu(Gly)₂ complex when bound to Cu²⁺. The individual conditional affinities of each glycine binding event (K_{a1} and K_{a2}), at pH 7.4, are 7.4×10^5 and 7.4×10^4 M^{-1}, respectively.[22]

The concentration of Gly required for equal mole equivalents of Cu²⁺ to be bound to both peptide and glycine is used to determine the affinity (conditional dissociation constants) at pH 7.4 of Cu²⁺ for the protein using eq 1. The "free" Cu²⁺ refers to the concentration of Cu²⁺ not bound to either glycine or peptide.

$$K_d = [Cu^{2+}_{free}] = \frac{[Cu^{2+}_{total}] - [Cu^{2+}_{bound\ to\ peptide}]}{1 + (K_{a1}[Gly_{free}]) + (K_{a1}K_{a2}([Gly_{free}]^2))}$$

(1)

where Cu²⁺ bound to peptide is equal to total Cu²⁺ (at θ = 0.5) divided by 2, and $[Gly_{free}] = [Gly_{total}] - [Gly_{bound\ to\ Cu^{2+}}]$.

■ RESULTS

Cu²⁺ Affinity of αSyn and Peptide Models. The Cu²⁺ affinity of the four peptides that model aspects of Cu²⁺ coordination to αSyn were studied. The affinities were determined at pH 7.4 using glycine as a competitive ligand

Table 1. Comparison of Cu^{2+} Binding Affinities and Wavelength Absorption Properties for αSyn and Model Peptides

protein/peptide	$K_d{}^a$ at pH 7.4	λ max absorption	λ max CD
αSyn(1−140)	0.1 nM	628 nm (pH 5.5−9)	610 nm (+)
MDV	0.28 nM	628 nm (pH 5.5−9)	618 nm (+)
αSyn(1−7,46−52)	0.03 nM	605 nm (pH 7.5−9)	570 nm (+) (pH 7.5−9)
		628 nm (pH 5.5)	610 nm (pH 5.5)
MAV	36 nM		555 nm (−)
αSyn(ac46−52)	18 000 nM	590 nm	525 nm (+)

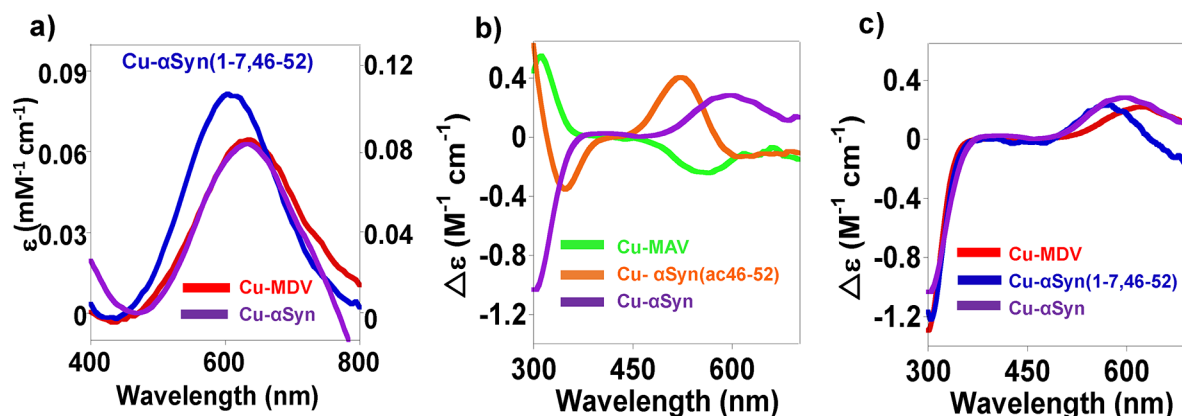$^a K_d$ is conditional dissociation constant, at pH 7.4; spectra reported at pH 7.4 unless stated.

Figure 3. Cu^{2+} visible absorption and vis-CD spectra of model peptides compared with full-length αSyn. (a) Visible absorbance spectra of αSyn (purple) compared with MDV (red) and αSyn(1−7,46−52) (blue). (The y-axis for αSyn is shown on right). (b) Vis-CD spectra of MAV (green) shown with αSyn(ac46−52) (orange) and αSyn (purple). (c) Vis-CD spectra MDV (red) compared to aαSyn(1−7,46−52) (blue) and αSyn (purple). All spectra are shown at pH 7.4, protein concentration 100−500 μM, 0.9 mol equiv of Cu^{2+}. Spectra of full-length αSyn have the closest similarity with the MDV peptide.

and directly compared to full-length αSyn (Figure 2, Table 1). The amount of glycine needed to compete Cu^{2+} from the αSyn peptides can be used to calculate the affinity by monitoring the visible-CD signal of Cu^{2+} bound to the αSyn peptides. This approach has the advantage of directly monitoring the coordination of Cu^{2+} to the model peptides, while the Cu(Gly)$_2$ complex is CD-silent and has a known affinity for Cu^{2+}. We note that there is no shift in wavelength of the absorption bands upon addition of glycine, which indicates a ternary complex is not favored, and so glycine is a direct competitor for Cu^{2+}. The difference in affinity for the four peptide models is quite marked. In particular, 8.5 mol equiv of glycine is required to remove half of the Cu^{2+} from MDV tripeptide (Figure 2a), while only 1.2 mol equiv of glycine is required to remove half of the Cu^{2+} from MAV (Figure 2c). Using eq 1 (see Experimental) a conditional dissociation constant (K_d) at pH 7.4 can be calculated. Cu^{2+} affinities for the various peptide models are summarized in Table 1. The conditional dissociation constants, at pH 7.4, range between 30 pM and 18 μM. Notably, the Cu^{2+} complex at the N-terminus involving Asp2 and chelation from histidine imidazole is an order of magnitude tighter, at 0.03 nM compared to the N-terminal tripeptide complex MDV, 0.3 nM. In contrast, the peptide that contains just His50 as a residue with a Cu^{2+} coordinating side chain has an affinity for Cu^{2+} 6 orders of magnitude weaker with a K_d of 18 μM.

The Cu^{2+} affinities for the four peptide models can be directly compared to full-length αSyn, Figure 2e. The affinity for full-length αSyn is slightly tighter than that of the tripeptide MDV, 0.3 nM, compared to 0.1 nM for full-length αSyn, while the peptide containing a histidine to form a macrochelate has an affinity 3 times tighter (0.03 nM) than full-length αSyn. To

summarize, the Cu^{2+} affinity for full-length αSyn is closest in magnitude to two model peptides, namely, MDV and the macrochelate complex MDV with the additional histidine residue, Table 1.

Visible Absorbance and CD Spectra. Next we compared the visible absorbance spectra and visible-CD spectra of the model peptides to full-length αSyn. The difference in Cu^{2+} coordination geometries is reflected in the visible absorbance spectra shown for Cu^{2+} loaded at 0.9 mol equiv, at pH 7.4, Figure 3a. In particular, an increase in the number of coordinating nitrogens in the Cu^{2+} tetragonal complex will result in absorbance maxima at shorter wavelengths, for the d−d electronic transitions. For example, absorbance bands range from 540 nm for the 4N complexes to 765 nm for a 1N3O complex.[23] This behavior is observed for the αSyn model peptides; the MDV Cu^{2+} complex was shown to form a 2N2O complex (Figure 1a) and has an absorption band centered at 630 nm, as would be predicted, while the macrochelate complex αSyn(1−7,46−52), which forms a 3N1O coordination (Figure 1b) is shifted to shorter wavelengths and has an absorption maximum at 605 nm, see Figure 3a. The absorption spectrum of full-length αSyn is almost identical to that of the absorbance spectrum for MDV, Figure 3a.

Visible-CD spectra are very sensitive to coordination geometry around Cu^{2+} and so can give additional information beyond the visible absorbance spectra, while not being complicated by signal from the presence of unbound Cu^{2+}.[10a,13] The visible-CD spectra of all four peptides are shown in Figure 3b,c, loaded with 0.9 mol equiv of Cu^{2+} at pH 7.4, and compared with full-length αSyn. The MDV analogue, with an Asp2Ala substitution, has marked effects on the CD spectra, causing an inversion of the vis-CD spectra for the d−d
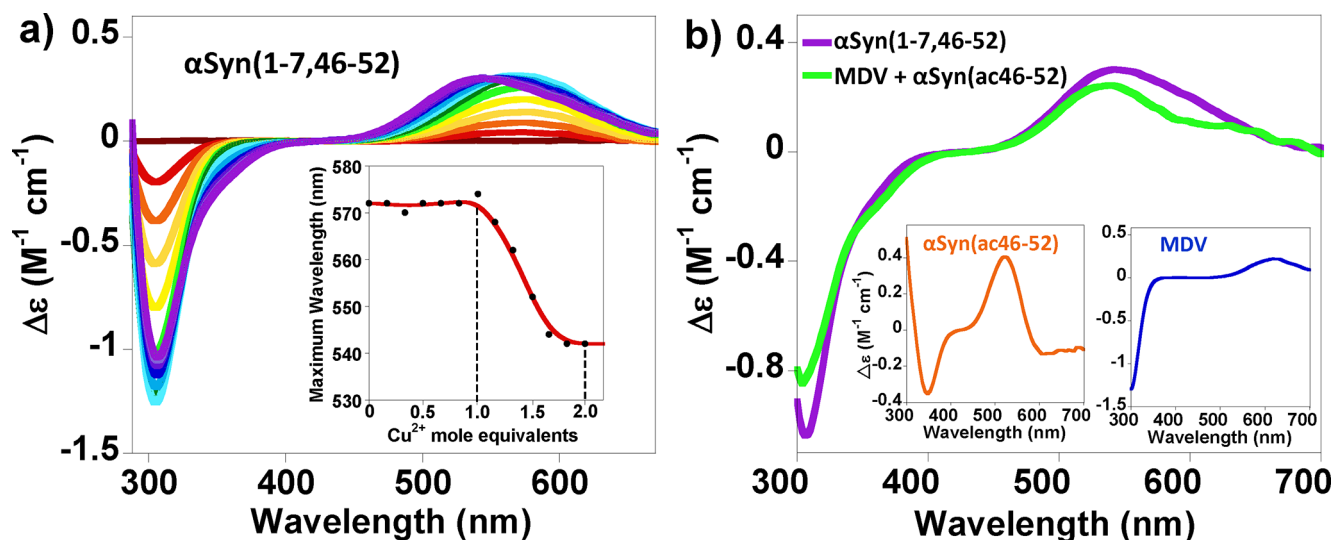
Figure 4. Cu^{2+} titration of the model peptide αSyn(1−7,46−52). (a) Vis-CD of Cu^{2+} titration up to 2 mol equiv. (inset) The shift in wavelength of the CD band from 570 to 540 nm between 1 and 2 Cu^{2+} equivalents. (b) Comparison of αSyn(1−7,46−52) with 2 equiv of Cu^{2+} compared to a simulated spectra created by the addition of spectra of MDV and αSyn(ac46−52) at 1 mol equiv, shown as insert. The macrochelate complex at 1 mol equiv (570 nm) is replaced by two independent complexes at the N-terminus and at the histidine above 1 equiv. Spectra recorded at pH 7.4, 25 °C, using 600 μM peptides.
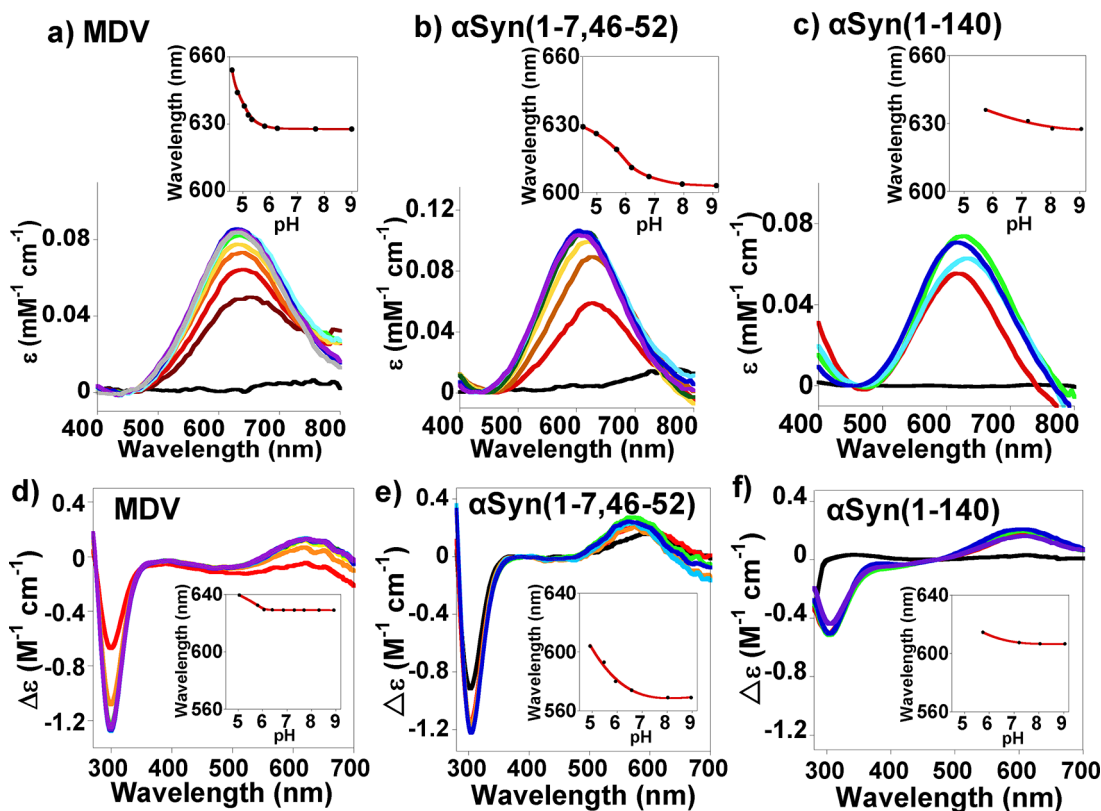

Figure 5. pH-dependent Cu^{2+} visible absorption and vis-CD spectra of model peptides compared with full-length αSyn. Visible absorbance spectra of (a) MDV, 500 μM; (b) αSyn(1−7,46−52) 500 μM; (c) full-length αSyn(1−140) 100 μM. Complementary vis-CD spectra of (d) MDV; (e) αSyn(1−7,46−52); (f) full-length αSyn. Spectra are shown between pH 4.5 and 9, 0.9 mol equiv of Cu^{2+}. pH-dependent spectra of full-length αSyn have the closest similarity with the MDV peptide, with no changes between pH 5.5 and 9 in contrast to αSyn(1−7,46−52).

electronic transition, as previously reported.[15a] Although not identical, the spectrum of αSyn has the closest similarity with MDV, with CD bands centered at 610 and 625 nm, respectively, Figure 3c. The visible-CD spectrum of αSyn(1−7,46−52), which can form the macrochelate with the histidine

side chain, also has similarities to full-length, but like the absorption spectrum the CD band is shifted to a shorter wavelength, with a visible-CD maxima at 570 nm. The CD signal of the αSyn(ac46−52) model peptide is very different
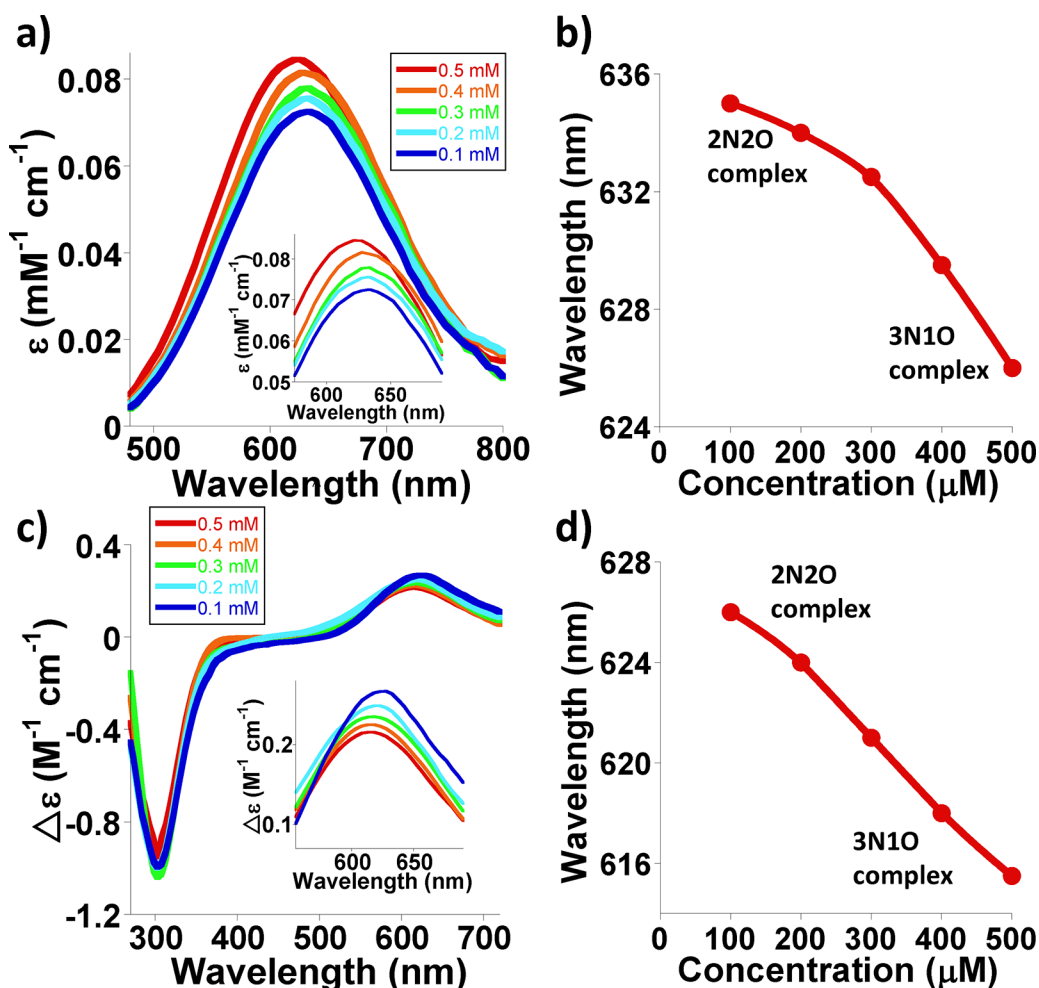
Figure 6. Concentration dependence of MDV ternary Cu^{2+} complex. Visible absorption (a) and vis-CD spectra (c) of MDV + αSyn(ac46−52) + Cu^{2+} (1:1:0.8 molar ratio). Spectra are shown over a range of concentrations, 100−500 μM, at pH 7.4. The associated change in wavelength maximum with concentration is also shown (b, d). The shift to shorter wavelengths at higher concentrations indicates the displacement of water with imidazole at higher concentrations.

with a positive CD band at 540 nm. The CD absorbance bands observed are also summarized in Table 1.

Stoichiometry of Cu^{2+} Coordination. To further probe the Cu^{2+} coordination to the model peptides, Cu^{2+} has been loaded onto the peptides beyond 1 mol equiv. Titration of Cu^{2+} onto MDV and MAV at pH 7.4 shows a clear 1:1 stoichiometry with fixed CD bands, centered at 612 and 555 nm, respectively, that increase in intensity until saturation at 1 mol equiv, shown in Supporting Information Figure S1a,b. Similarly, the αSyn(ac46−52) peptide also forms a 1:1 complex with a single set of CD signal at 520 and 320 nm (Supporting Information Figure S1c). In contrast, the Cu^{2+} binding properties of αSyn(1−7,46−52) are more complicated with a CD band at 573 nm that increases in intensity up to 1 mol equiv of Cu^{2+}; this CD band then reduces a little in intensity, while a CD band centered at 543 nm appears, Figure 4a. Addition of a second Cu^{2+} ion shifts the CD band toward a shorter wavelength of 543 nm; this change in wavelength maxima in the CD spectra between 1 and 2 mol equiv of Cu^{2+} is shown as an inset in Figure 4a. We postulated that the macrochelate complex composed of the N-terminus and histidine is replaced by two separate complexes at 2 equiv of Cu^{2+}, with the two separate complexes centered at MDV and His50, as previously suggested.[17] This possible behavior is

strongly supported by simulated data presented in Figure 4b; here the spectrum of αSyn(1−7, 46−52) with 2 equiv of Cu^{2+} can be very closely mimicked by the direct combination of two individual CD spectra of MDV and αSyn(ac46−52) at 1 equiv, as shown in Figure 4b. This Cu^{2+} titration indicates the coordination geometry is sensitive to changes in Cu^{2+} stoichiometry with loss of the macrochelate at supra-stoichiometric equivalents.

pH Dependence of Cu^{2+} Binding: Histidine Coordination Is Lost at Low pH. The pH dependence of Cu^{2+} binding to the MDV tripeptide and αSyn(1−7,46−52) is shown in Figure 5. These are highlighted, because they have the most similar CD, absorbance spectra, and affinity to full-length αSyn, which is also shown in Figure 5. Figure 5a−c shows visible absorption spectra, while Figure 5d−f shows the complementary visible-CD spectra over a range of pH values in the presence of 1 mol equiv of Cu^{2+}. A single set of visible-CD bands for MDV remains very stable over a range of pHs (between pH 5 and 10); there is no indication of a shift to other coordination geometries with an increase in pH. The midpoint of Cu^{2+} complex formation occurs at a relatively low pH of 4.6 for MDV (Figure 5a). Clearly, the Asp has a significant stabilizing influence on the complex even at relatively low pH values, as previously described.[15a]

The behavior of αSyn(1−7,46−52) coordination is more complex. At pH 7 and above the visible absorption spectra are consistent with a 3N1O geometry, which has an absorbance maximum at 600 nm. Below pH 7 the absorbance maxima shifts to longer wavelengths from 600 to 630 nm, Figure 5b, which is consistent with 2N2O coordination. This shift to longer wavelengths at lower pH values is echoed in the visible-CD spectra, which shift from 605 to 630 nm for the CD bands, Figure 5e. The αSyn(1−7,46−52) visible-CD bands below pH 6 adopt the same appearance as the MDV tripeptide. This suggests a change in coordination from 3N1O complex (pH 7.0) to a 2N2O complex at lower pH (pH 5.5). This behavior indicates the loss of the macrochelate imidazole ligand between pH 5.5 and 7. The pH dependence spectra of full-length αSyn resembles much more closely the behavior of MDV than the αSyn(1−7,46−52) peptide. In particular, there is no marked-shift in absorbance maximum between pH 7 and 5.5. Like the MDV tripeptide the absorbance bands remain centered at 630 nm over the whole range of pH for full-length αSyn. This is strong evidence to rule out any significant role for coordination by His50 in full-length αSyn Cu^{2+} complex even at high pH.

The pH-dependent vis-CD spectra of Cu^{2+} complexes for MAV is shown as Supporting Information, Figure S2, and they are very different from the behavior of full-length αSyn. In the case of MAV, which lacks aspartate, the vis-CD spectra suggest a complete loss of amide Cu^{2+} coordination below pH 7, with a midpoint at pH 7.5. This type of pH dependence for MAV is similar to the tripeptide AAA.[12b] The αSyn(ac46−52) Cu^{2+} complex is also very pH-sensitive, with the loss of a CD active complex below pH 6 implying a loss of amide main-chain coordination, Supporting Information Figure S2b.

Concentration Dependence of Imidazole Chelation to the N-Terminal Cu^{2+} Complex. Our absorption and visible-CD data indicate the His50 does not bind to the N-terminal Cu^{2+} complex in full-length αSyn, and yet there are two quite careful studies using multipulse electron para-magnetic resonance (EPR) to indicate His50 does coordinate in full-length αSyn.[16a,b] We wondered how these conflicting observations could be reconciled. We postulated that the differences observed might be related to the differences in experimental conditions. In particular, the EPR spectra were acquired at much higher concentrations in the presence of the cryo-protectant glycerol. We questioned if the glycerol might impact the αSyn structure and its ability to form a macrochelate. We therefore obtained visible-CD and absorbance spectra of Cu^{2+}-loaded αSyn in the presence of 25% (v/v) glycerol. Comparison of the absorption spectra and visible-CD indicate glycerol does not affect the coordination of the Cu^{2+}, see Supporting Information Figure S3, which rules this out as an explanation of the conflicting binding modes reported.

Next, we determined whether higher concentrations (350 μM) used in the EPR experiments could explain the different behavior. Full-length αSyn is poorly soluble, so it was not possible to study using optical spectroscopy; however, it was possible to use the more soluble MDV model peptide over a range of concentrations between 500 (used in the EPR experiments) and 100 μM used here in the visible absorption/CD experiments. We studied the ternary complex of MDV/Cu^{2+}/αSyn(ac46−52) (1:1:1) over a range of concentrations. A clear concentration dependence of the wavelength maxima in both the visible-absorption and visible-CD spectra is observed, Figure 6. We also show a very similar concentration-dependent behavior for the mixture of MDV/

imidazole/Cu^{2+} (1:1:1), shown as Supporting Information Figure S4. The impact of imidazole on the Cu-MDV visible absorption spectra is also shown in Supporting Information Figure S5. This ternary 3N1O complex with imidazole has previously been described.[17] Our spectra indicate, the more concentrated the (1:1:1) mixture, the more the absorbance bands shifted to shorter wavelengths. The shift to shorter wavelengths at higher concentrations suggests an increase in the extent of nitrogen (imidazole) equatorial chelation as the water oxygen is displaced. The concentration-dependent behavior of the ternary complex, Figures 6 and S4, gives an explanation for the differing reports of His50 involvement in the N-terminal complex of full-length αSyn.

To confirm a role for the imidazole chelation of Cu^{2+} at higher concentrations, control experiments were performed with MDV and Cu^{2+} only. As expected the spectra show no concentration-dependent behavior, Supporting Information Figure S6. We also performed concentration-dependent measurements for αSyn(1−7,46−52), Supporting Information Figure S7. This peptide exhibits absorbance bands typical for a 3N1O complex over all concentrations. This concentration-independent behavior supports the assertion that αSyn(1−7,46−52), with just 12 amino acids between the histidine and the N-terminus, forms a macrochelate rather than a ternary complex.

■ DISCUSSION

To resolve controversies surrounding Cu^{2+} coordination to αSyn we compared affinity, visible absorbance, visible CD, and pH dependence behavior for full-length αSyn to that of a series of model peptides. Taking these data together, the peptide model that most closely mimics Cu^{2+} binding to full-length αSyn is that of the simple tripeptide MDV, Figure 7a. The lack of pH dependence changes of full-length αSyn for visible absorbance and visible CD spectra rules out the formation of the complex with His50. In contrast, αSyn(1−7,46−52) does have imidazole nitrogen coordination at pH 7.4, which begins to be lost at pH values below 7 and is completely lost by pH 5.5, Figure 7b. The different behavior of αSyn(1−7,46−52)
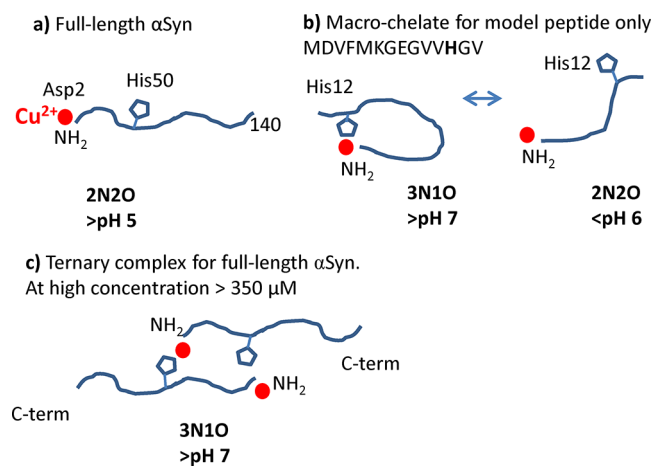

a) Full-length αSyn

Asp2   His50

Cu^{2+}●
  NH$_2$ 140

2N2O
>pH 5

b) Macro-chelate for model peptide only
MDVFMKGEGVVHGV

His12   His12

His12 ↔

  NH$_2$ NH$_2$

3N1O   **2N2O**
>pH 7   **<pH 6**

c) Ternary complex for full-length αSyn.
At high concentration > 350 μM

  NH$_2$
              C-term
      NH$_2$

C-term

3N1O
>pH 7

Figure 7. Primary Cu^{2+} binding site for αSyn. (a) Cu^{2+} binds to the N-terminus independently from His50 in full-length αSyn. (b) Only model peptides with histidine close in sequence to the N-terminus (αSyn(1−7,46−52)) form the macrochelate, 3N1O complex at pH > 7.0. (c) Ternary complex possible with His50 at high concentrations greater than 350 μM but not a macrochelate.

model peptide compared to full-length αSyn can be explained by the considerable reduction in the number of residues between the N-terminus and the histidine to just 12 residues in the model peptide. This facilitates histidine side-chain coordination in the N-terminal complex. We show here that higher pH and substoichiometric ratios of Cu^{2+} will promote the macrochelate in the model peptide αSyn(1−7,46−52); however, even under these conditions our data indicate the His50 macrochelate does not form for full-length αSyn. The visible absorption spectra are essentially identical for Cu^{2+} bound to MDV and full-length αSyn over the entire pH range of 5−9. There are however subtle differences in the Cu^{2+} vis-CD spectra; these may reflect very small differences in the conformation of the main chain in the plain of the copper complex,[12] caused by the presence of the additional 140 residues, rather than differences in the coordinating ligands. The involvement of His50 (at 100 μM αSyn) can be ruled out, as there are no pH-dependent changes in coordination between pH 5.5 and 7.

So why have some studies reported His50 involvement in the primary N-terminal Cu^{2+} complex? There are two key studies using EPR and full-length αSyn that suggest this involvement.[16a,b] Drew et al. points to a mixture of both 3N1O and 2N2O coordination geometries (Figure 1a,b) in approximately equal proportions at pH 7.4.[16a] Their relative proportions are likely to be pH-sensitive; indeed, an EPR study at pH 6.5 indicates a single set of EPR signals for the 2N2O complex.[15a] An explanation for the different observations compared to the data presented here simply arises from the experimental condition, when acquiring EPR spectra. In particular, the EPR spectra are acquired at 350 μM of αSyn; these high concentrations favor displacement of the water with His50 imidazole from a second αSyn molecule, Figure 7c. This assertion is supported by the concentration-dependent behavior of the model ternary system (MDV + αSyn(ac46−52) + Cu^{2+}) shown in Figure 6. Only at the higher concentrations can the imidazole displace the water. This concentration-dependent behavior can explain the change in coordination from 2N2O at low concentration to 3N1O at higher concentration. This also suggests that rather than full-length αSyn forming a macrochelate, whose formation would be independent of concentration, the His50 coordination is derived from a second αSyn molecule only favored at higher concentrations.

We note that, in full-length αSyn, His50 is covalently linked to the N-terminus, and this will increase the "effective concentration" of His50 close to the N-terminus in this intrinsically disordered protein. However, this is not sufficient to overcome the significant ordering necessary to form the macrochelate across 50 residues. Only by raising the actual concentration of αSyn can coordination by His50 take place from a second αSyn molecule coordinating to the N-terminal Cu^{2+} complex forming a ternary complex, rather than the formation of a macrochelate, Figure 7c. Our data indicate that at 100 μM and below the proportion of His50 chelation at the N-terminal Cu^{2+} complex will be minimal. Although the 3N1O complex (ternary or macrochelate) could also be present in small amounts, at physiological concentrations the 2N2O complex dominates (Figure 1a).

Others have described His50 involvement at pH 6.5;[16c] we suggest that, in this case, the interpretation of the data is incorrect. The study points to a 2N2O Cu^{2+} complex as seen in the MDV complex but suggests that the nitrogen ligand is from

His50 rather than the N-terminal amino group.[16c] This type of complex is extremely unlikely; there is a large body of evidence for αSyn, along with many other Cu^{2+} protein complexes, that points to the N-terminal amino group anchoring Cu^{2+} complexes.[24] In particular, acetylation of the N-terminal amino group completely removes the strong coordination mode from αSyn.[20]

The concentration-dependent behavior we identified suggests that, at physiological concentrations of αSyn, His50 will not bind at the N-terminal complex; however, self-association of αSyn might favor the ternary Cu^{2+} complex formation. This in turn will influence the αSyn fibril assembly pathway[8] and morphology.[9a,b] Recent high-resolution cryo-EM structures of αSyn indicate that the His50 is distant from the N-terminus in the final fibril structures reported,[25] even when you consider bridging ternary Cu^{2+} complexes between two αSyn molecules in the fibril structure.

The affinity of Cu^{2+} for αSyn is an important determinant of the physiological relevance of the interaction. Cu^+ is tightly chaperoned and regulated within the cytosol, while Cu^{2+} is more weakly bound extracellularly, and it is believed Cu^{2+} reaches levels of 15 μM;[26] some have reported even higher fluxes of Cu^{2+} at the synapse, from 20 to 250 μM, during neuronal depolarization.[27] The 0.1 nM affinity (K_d) determined here for αSyn is therefore sufficiently tight to bind extracellular levels of Cu^{2+}.

The affinity measured here of 0.1 nM conditional dissociation constant for full-length αSyn at pH 7.4 (and for MDV 0.28 nM) is in agreement with a number of studies on full-length αSyn using a range of techniques: 0.2 nM at pH 7.4;[28] 0.1 nM at pH 7.4;[16b] and 0.4 nM at pH 7.0.[5b] Others have reported affinities weaker than the 0.1 nM,[15a,29] but none have suggested an affinity (K_d) as tight as 0.03 nM observed for the model peptide αSyn(1−7,46−52), which can form the macrochelate with histidine. This further supports our assertion that Histidine50 does not stabilize the primary Cu^{2+} binding site in monomeric αSyn.

The affinity for our acetylated peptide containing a single histidine, αSyn(ac46−52), was determined to have a K_d of 18 μM at pH 7.4, which is in agreement with other reports.[30] This peptide represents a model for Cu^{2+} binding to full-length acetylated αSyn. The N-terminally acetylated peptide has a Cu^{2+} affinity 5 orders of magnitude weaker than nonacetylated αSyn.

■ CONCLUSION

We have shown that free imidazole or His50 within αSyn will only displace water as a ligand to the N-terminal Cu^{2+} complex at high (>350 μM) concentrations. This concentration-dependent behavior gives an explanation for the seemingly conflicting observations made regarding the role of His50. Our studies show that, although αSyn is intrinsically disordered, forming a large macrochelate is not favored. Cu^{2+} coordination to the N-terminus together with His50 only takes place at higher, nonphysiological, concentrations (used in EPR measurements), which results in a ternary complex, Figure 7c.

Cu^{2+} coordination to αSyn and its N-terminal acetylated form has been shown to accelerate fibril assembly.[8,10] Cu^{2+} binding to the N-terminus can also impact the assembly pathway,[8] fibril morphology,[9a−c] and cytotoxicity[9b,c] of αSyn. How changes in metal homeostasis can impact the development of Parkinson's disease is still an open question.[2,3] We still have much to discover surrounding the role of physiological

metal ions in the amyloid assembly, redox chemistry, and cytotoxicity of αSyn and other amyloidogenic proteins.

ASSOCIATED CONTENT

Ⓢ Supporting Information

The Supporting Information is available free of charge on the ACS Publications website at DOI: 10.1021/acs.inorgchem.9b02644.

Spectra showing stoichiometry, metal ion binding, pH dependence, concentration dependence (PDF)

AUTHOR INFORMATION

Corresponding Author

*E-mail: j.viles@qmul.ac.uk

ORCID 🄳

Giuliana Fusco: 0000-0002-3644-9809

John H. Viles: 0000-0001-7533-2964

Author Contributions

‖Authors have contributed equally to this manuscript.

Notes

The authors declare no competing financial interest.

REFERENCES

(1) (a) Polymeropoulos, M. H.; Lavedan, C.; Leroy, E.; Ide, S. E.; Dehejia, A.; Dutra, A.; Pike, B.; Root, H.; Rubenstein, J.; Boyer, R.; Stenroos, E. S.; Chandrasekharappa, S.; Athanassiadou, A.; Papapetropoulos, T.; Johnson, W. G.; Lazzarini, A. M.; Duvoisin, R. C.; DiIorio, G.; Golbe, L. I.; Nussbaum, R. L. Mutation in the alpha-synuclein gene identified in families with Parkinson's disease. *Science* **1997**, *276* (5321), 2045−2047. (b) Kruger, R.; Kuhn, W.; Muller, T.; Woitalla, D.; Graeber, M.; Kosel, S.; Przuntek, H.; Epplen, J. T.; Schols, L.; Riess, O. Ala30Pro mutation in the gene encoding alpha-synuclein in Parkinson's disease. *Nat. Genet.* **1998**, *18* (2), 106−108. (c) Appel-Cresswell, S.; Vilarino-Guell, C.; Encarnacion, M.; Sherman, H.; Yu, I.; Shah, B.; Weir, D.; Thompson, C.; Szu-Tu, C.; Trinh, J.; Aasly, J. O.; Rajput, A.; Rajput, A. H.; Stoessl, A. J.; Farrer, M. J. Alpha-synuclein p.H50Q, a novel pathogenic mutation for Parkinson's disease. *Mov. Disord.* **2013**, *28* (6), 811−813.

(2) Pall, H. S.; Blake, D. R.; Gutteridge, J. M.; Williams, A. C.; Lunec, J.; Hall, M.; Taylor, A. RAISED CEREBROSPINAL-FLUID COPPER CONCENTRATION IN PARKINSON'S DISEASE. *Lancet* **1987**, *330* (8553), 238−241.

(3) Gorell, J.; Johnson, C.; Rybicki, B.; Peterson, E.; Kortsha, G.; Brown, G.; Richardson, R. Occupational exposure to manganese, copper, lead, iron, mercury and zinc and the risk of Parkinson's disease. *Neurotoxicology* **1998**, *20* (2−3), 239−247.

(4) (a) Binolfi, A.; Valiente-Gabioud, A. A.; Duran, R.; Zweckstetter, M.; Griesinger, C.; Fernandez, C. O. Exploring the Structural Details of Cu(I) Binding to alpha-Synuclein by NMR Spectroscopy. *J. Am. Chem. Soc.* **2011**, *133* (2), 194−196. (b) Binolfi, A.; Quintanar, L.; Bertoncini, C. W.; Griesinger, C.; Fernández, C. O. Bioinorganic chemistry of copper coordination to alpha-synuclein: Relevance to Parkinson's disease. *Coord. Chem. Rev.* **2012**, *256* (19−20), 2188−2201. (c) Valensin, D.; Dell'Acqua, S.; Kozlowski, H.; Casella, L. Coordination and redox properties of copper interaction with alpha-synuclein. *J. Inorg. Biochem.* **2016**, *163*, 292−300.

(5) (a) Wang, C.; Liu, L.; Zhang, L.; Peng, Y.; Zhou, F. Redox Reactions of the α-Synuclein−Cu2+ Complex and Their Effects on Neuronal Cell Viability. *Biochemistry* **2010**, *49* (37), 8134−8142. (b) Davies, P.; Wang, X.; Sarell, C. J.; Drewett, A.; Marken, F.; Viles, J. H.; Brown, D. R. The Synucleins Are a Family of Redox-Active Copper Binding Proteins. *Biochemistry* **2011**, *50* (1), 37−47.

(c) Meloni, G.; Vašák, M. Redox activity of α-synuclein−Cu is silenced by Zn7-metallothionein-3. *Free Radical Biol. Med.* **2011**, *50* (11), 1471−1479.

(6) (a) Abeyawardhane, D. L.; Fernandez, R. D.; Heitger, D. R.; Crozier, M. K.; Wolver, J. C.; Lucas, H. R. Copper Induced Radical Dimerization of alpha-Synuclein Requires Histidine. *J. Am. Chem. Soc.* **2018**, *140* (49), 17086−17094. (b) Al-Hilaly, Y. K.; Biasetti, L.; Blakeman, B. J. F.; Pollack, S. J.; Zibaee, S.; Abdul-Sada, A.; Thorpe, J. R.; Xue, W. F.; Serpell, L. C. The involvement of dityrosine crosslinking in alpha-synuclein assembly and deposition in Lewy Bodies in Parkinson's disease. *Sci. Rep.* **2016**, *6*, 39171. (c) Gu, M.; Bode, D. C.; Viles, J. H. Copper Redox Cycling Inhibits A beta Fibre Formation and Promotes Fibre Fragmentation, while Generating a Dityrosine A beta Dimer. *Sci. Rep.* **2018**, *8*, 16190.

(7) (a) Borghi, R.; Marchese, R.; Negro, A.; Marinelli, L.; Forloni, G.; Zaccheo, D.; Abbruzzese, G.; Tabaton, M. Full length alpha-synuclein is present in cerebrospinal fluid from Parkinson's disease and normal subjects. *Neurosci. Lett.* **2000**, *287* (1), 65−67. (b) Lee, S. J. Origins and effects of extracellular alpha-synuclein: Implications in Parkinson's disease. *J. Mol. Neurosci.* **2008**, *34* (1), 17−22.

(8) Zhang, H. Y.; Griggs, A.; Rochet, J. C.; Stanciu, L. A. In Vitro Study of alpha-Synuclein Protofibrils by Cryo-EM Suggests a Cu2+-Dependent Aggregation Pathway. *Biophys. J.* **2013**, *104* (12), 2706−2713.

(9) (a) Uversky, V. N.; Li, J.; Fink, A. L. Metal-triggered Structural Transformations, Aggregation, and Fibrillation of Human α-Synuclein: A POSSIBLE MOLECULAR LINK BETWEEN PARKINSON'S DISEASE AND HEAVY METAL EXPOSURE. *J. Biol. Chem.* **2001**, *276* (47), 44284−44296. (b) Wright, J. A.; Wang, X.; Brown, D. R. Unique copper-induced oligomers mediate alpha-synuclein toxicity. *FASEB J.* **2009**, *23* (8), 2384−2393. (c) Choi, T. S.; Lee, J.; Han, J. Y.; Jung, B. C.; Wongkongkathep, P.; Loo, J. A.; Lee, M. J.; Kim, H. I. Supramolecular Modulation of Structural Polymorphism in Pathogenic -Synuclein Fibrils Using Copper(II) Coordination. *Angew. Chem., Int. Ed.* **2018**, *57* (12), 3099−3103.

(10) (a) Rasia, R. M.; Bertoncini, C. W.; Marsh, D.; Hoyer, W.; Cherny, D.; Zweckstetter, M.; Griesinger, C.; Jovin, T. M.; Fernández, C. O. Structural characterization of copper(II) binding to α-synuclein: Insights into the bioinorganic chemistry of Parkinson's disease. *Proc. Natl. Acad. Sci. U. S. A.* **2005**, *102* (12), 4294−4299. (b) Binolfi, A.; Rasia, R. M.; Bertoncini, C. W.; Ceolin, M.; Zweckstetter, M.; Griesinger, C.; Jovin, T. M.; Fernandez, C. O. Interaction of alpha-synuclein with divalent metal ions reveals key differences: A link between structure, binding specificity and fibrillation enhancement. *J. Am. Chem. Soc.* **2006**, *128* (30), 9893−9901. (c) Abeyawardhane, D. L.; Heitger, D. R.; Fernandez, R. D.; Forney, A. K.; Lucas, H. R. C-Terminal Cu-II Coordination to alpha-Synuclein Enhances Aggregation. *ACS Chem. Neurosci.* **2019**, *10* (3), 1402−1410.

(11) Viles, J. H. Metal ions and amyloid fiber formation in neurodegenerative diseases. Copper, zinc and iron in Alzheimer's, Parkinson's and prion diseases. *Coord. Chem. Rev.* **2012**, *256* (19−20), 2271−2284.

(12) (a) Martin, R. B. Optical properties of transition metal ion complexes of amino acids and peptides. *Metal ions in biological systems* **1974**, *1*, 129−156. (b) Stanyon, H. F.; Cong, X. J.; Chen, Y.; Shahidullah, N.; Rossetti, G.; Dreyer, J.; Papamokos, G.; Carloni, P.; Viles, J. H. Developing predictive rules for coordination geometry from visible circular dichroism of copper(II) and nickel(II) ions in histidine and amide main-chain complexes. *FEBS J.* **2014**, *281* (17), 3945−3954. (c) Klewpatinond, M.; Viles, J. H. Empirical rules for rationalising visible circular dichroism of Cu(2+) and Ni(2+) histidine complexes: Applications to the prion protein. *FEBS Lett.* **2007**, *581* (7), 1430−1434.

(13) (a) Klewpatinond, M.; Davies, P.; Bowen, S.; Brown, D. R.; Viles, J. H. Deconvoluting the Cu2+ Binding Modes of Full-length Prion Protein. *J. Biol. Chem.* **2008**, *283* (4), 1870−1881. (b) Viles, J. H.; Cohen, F. E.; Prusiner, S. B.; Goodin, D. B.; Wright, P. E.; Dyson, H. J. Copper binding to the prion protein: Structural implications of four identical cooperative binding sites. *Proc. Natl. Acad. Sci. U. S. A.*

1999, *96* (5), 2042−2047. (c) Stanyon, H. F.; Patel, K.; Begum, N.; Viles, J. H. Copper(II) Sequentially Loads onto the N-Terminal Amino Group of the Cellular Prion Protein before the Individual Octarepeats. *Biochemistry* **2014**, *53* (24), 3934−3939.

(14) Sung, Y. H.; Rospigliosi, C.; Eliezer, D. NMR mapping of copper binding sites in alpha-synuclein. *Biochim. Biophys. Acta, Proteins Proteomics* **2006**, *1764* (1), 5−12.

(15) (a) Binolfi, A. s.; Rodriguez, E. E.; Valensin, D.; D'Amelio, N.; Ippoliti, E.; Obal, G.; Duran, R.; Magistrato, A.; Pritsch, O.; Zweckstetter, M.; Valensin, G.; Carloni, P.; Quintanar, L.; Griesinger, C.; Fernandez, C. O. Bioinorganic Chemistry of Parkinson's Disease: Structural Determinants for the Copper-Mediated Amyloid Formation of Alpha-Synuclein. *Inorg. Chem.* **2010**, *49* (22), 10668−10679. (b) Kowalik-Jankowska, T.; Rajewska, A.; Wiśniewska, K.; Grzonka, Z.; Jezierska, J. Coordination abilities of N-terminal fragments of *α*-synuclein towards copper(II) ions: A combined potentiometric and spectroscopic study. *J. Inorg. Biochem.* **2005**, *99* (12), 2282−2291. (c) Binolfi, A. s.; Lamberto, G. R.; Duran, R.; Quintanar, L.; Bertoncini, C. W.; Souza, J. M.; Cerveñansky, C.; Zweckstetter, M.; Griesinger, C.; Fernandez, C. O. Site-Specific Interactions of Cu(II) with *α* and *β*-Synuclein: Bridging the Molecular Gap between Metal Binding and Aggregation. *J. Am. Chem. Soc.* **2008**, *130* (35), 11801−11812.

(16) (a) Drew, S. C.; Ling Leong, S.; Pham, C. L. L.; Tew, D. J.; Masters, C. L.; Miles, L. A.; Cappai, R.; Barnham, K. J. Cu2+ Binding Modes of Recombinant *α*-Synuclein − Insights from EPR Spectroscopy. *J. Am. Chem. Soc.* **2008**, *130* (24), 7766−7773. (b) Dudzik, C. G.; Walter, E. D.; Millhauser, G. L. Coordination Features and Affinity of the Cu2+ Site in the *α*-Synuclein Protein of Parkinson's Disease. *Biochemistry* **2011**, *50* (11), 1771−1777. (c) Bortolus, M.; Bisaglia, M.; Zoleo, A.; Fittipaldi, M.; Benfatto, M.; Bubacco, L.; Maniero, A. L. Structural Characterization of a High Affinity Mononuclear Site in the Copper(II)-*α*-Synuclein Complex. *J. Am. Chem. Soc.* **2010**, *132* (51), 18057−18066. (d) Kowalik-Jankowska, T.; Rajewska, A.; Jankowska, E.; Grzonka, Z. Copper(II) binding by fragments of alpha-synuclein containing M-1-D-2- and -H-50-residues; a combined potentiometric and spectroscopic study. *Dalton T* **2006**, No. 42, 5068−5076.

(17) De Ricco, R.; Valensin, D.; Dell'Acqua, S.; Casella, L.; Dorlet, P.; Faller, P.; Hureau, C. Remote His50 Acts as a Coordination Switch in the High-Affinity N-Terminal Centered Copper(II) Site of alpha-Synuclein. *Inorg. Chem.* **2015**, *54* (10), 4744−4751.

(18) Ohrfelt, A.; Zetterberg, H.; Andersson, K.; Persson, R.; Secic, D.; Brinkmalm, G.; Wallin, A.; Mulugeta, E.; Francis, P. T.; Vanmechelen, E.; Aarsland, D.; Ballard, C.; Blennow, K.; Westman-Brinkmalm, A. Identification of Novel alpha-Synuclein Isoforms in Human Brain Tissue by using an Online NanoLC-ESI-FTICR-MS Method. *Neurochem. Res.* **2011**, *36* (11), 2029−2042.

(19) Bartels, T.; Choi, J. G.; Selkoe, D. J. alpha-Synuclein occurs physiologically as a helically folded tetramer that resists aggregation. *Nature* **2011**, *477* (7362), 107−U123.

(20) (a) Moriarty, G. M.; Minetti, C. A. S. A.; Remeta, D. P.; Baum, J. A Revised Picture of the Cu(II)-alpha-Synuclein Complex: The Role of N-Terminal Acetylation. *Biochemistry* **2014**, *53* (17), 2815−2817. (b) Miotto, M. C.; Valiente-Gabioud, A. A.; Rossetti, G.; Zweckstetter, M.; Carloni, P.; Selenko, P.; Griesinger, C.; Binolfi, A.; Fernandez, C. O. Copper Binding to the N-Terminally Acetylated, Naturally Occurring Form of Alpha-Synuclein Induces Local Helical Folding. *J. Am. Chem. Soc.* **2015**, *137* (20), 6444−6447.

(21) Fusco, G.; De Simone, A.; Gopinath, T.; Vostrikov, V.; Vendruscolo, M.; Dobson, C. M.; Veglia, G. Direct observation of the three regions in alpha-synuclein that determine its membrane-bound behaviour. *Nat. Commun.* **2014**, *5*, 3827.

(22) Dawson, R.; Elliott, D.; Elliott, W.; Jones, K. *Data for Biochemical Research,* 3rd ed.; Clarendon Press: Oxford, UK, 1986.

(23) Bryce, G. F.; Gurd, F. R. N. Visible Spectra and Optical Rotatory Properties of Cupric Ion Complexes of l-Histidine-containing Peptides. *J. Biol. Chem.* **1966**, *241* (1), 122−129.

(24) (a) Patel, S. U.; Sadler, P. J.; Tucker, A.; Viles, J. H. Direct-Detection of Albumin in Human Blood-Plasma by 1h Nmr-Spectroscopy - Complexation of Nickel2+. *J. Am. Chem. Soc.* **1993**, *115* (20), 9285−9286. (b) Barritt, J. D.; Viles, J. H. Truncated Amyloid-beta((11−40/42)) from Alzheimer Disease Binds Cu2+ with a Femtomolar Affinity and Influences Fiber Assembly. *J. Biol. Chem.* **2015**, *290* (46), 27791−27802.

(25) (a) Li, B. S.; Ge, P.; Murray, K. A.; Sheth, P.; Zhang, M.; Nair, G.; Sawaya, M. R.; Shin, W. S.; Boyer, D. R.; Ye, S. L.; Eisenberg, D. S.; Zhou, Z. H.; Jiang, L. Cryo-EM of full-length alpha-synuclein reveals fibril polymorphs with a common structural kernel. *Nat. Commun.* **2018**, *9*, 3609. (b) Guerrero-Ferreira, R.; Taylor, N. M. I.; Mona, D.; Ringler, P.; Lauer, M. E.; Riek, R.; Britschgi, M.; Stahlberg, H. Cryo-EM structure of alpha-synuclein fibrils. *Elife* **2018**, *7*, 36402.

(26) Hartter, D. E.; Barnea, A. Evidence for release of copper in the brain: depolarization-induced release of newly taken-up 67copper. *Synapse* **1988**, *2* (4), 412−5.

(27) (a) Kardos, J.; Kovacs, I.; Hajos, F.; Kalman, M.; Simonyi, M. Nerve endings from rat brain tissue release copper upon depolarization. A possible role in regulating neuronal excitability. *Neurosci. Lett.* **1989**, *103* (2), 139−44. (b) Brown, D. R.; Qin, K.; Herms, J. W.; Madlung, A.; Manson, J.; Strome, R.; Fraser, P. E.; Kruck, T.; von Bohlen, A.; Schulz-Schaeffer, W.; Giese, A.; Westaway, D.; Kretzschmar, H. The cellular prion protein binds copper in vivo. *Nature* **1997**, *390* (6661), 684−7.

(28) Hong, L.; Simon, J. D. Binding of Cu(II) to Human *α*-Synucleins: Comparison of Wild Type and the Point Mutations Associated with the Familial Parkinson's Disease. *J. Phys. Chem. B* **2009**, *113* (28), 9551−9561.

(29) Jackson, M. S.; Lee, J. C. Identification of the Minimal Copper(II)-Binding *α*-Synuclein Sequence. *Inorg. Chem.* **2009**, *48* (19), 9303−9307.

(30) Valensin, D.; Camponeschi, F.; Luczkowski, M.; Baratto, M. C.; Remelli, M.; Valensin, G.; Kozlowski, H. The role of His-50 of alpha-synuclein in binding Cu(II): pH dependence, speciation, thermodynamics and structure. *Metallomics* **2011**, *3* (3), 292−302.